Unambiguous DOA Estimation Using Multi-Frequency Rational Sparse Arrays

Md. Waqeeb T. S. Chowdhury and Yimin D. Zhang

Department of Electrical and Computer Engineering, Temple University, Philadelphia, PA 19122, USA

***Abstract*—In this paper, we consider the conditions for unique identifiability of the direction-of-arrival (DOA) estimation problem under a multi-frequency sparse rational array framework. Previous studies on the multi-frequency scenario involved integer locations of the virtual sensor locations at each frequency. The rational array framework removes such requirements and thus provides higher flexibility in multi-frequency sparse array design. We provide a generalized necessary condition for the unambiguous detection of signal DOAs in terms of the maximum spatial correlation coefficient between distinct signal directions, and the applicability of direct MUSIC for the unambiguous detection of signals exploiting rational sparse arrays is considered. The effectiveness of multi-frequency rational sparse arrays and the proposed analyses is verified using simulation results.**

Keywords: Direction-of-arrival estimation, sparse array, rational analysis, multi-frequency array design.

I. Introduction

Using antenna arrays for DOA estimation has attracted extensive research over the last several decades. Due to the requirement of the Nyquist sampling theorem, the most commonly used antenna array structure is the uniform linear array (ULA), which consists of linearly placed sensors with an inter-element spacing of half the signal wavelength [1]. However, ULAs are not efficient in terms of the offered degrees-of-freedom (DOFs) with respect to the number of physical sensors. For this reason, sparse arrays have recently gained high popularity [2–4]. Assuming the same number of L sensors, a spare linear array can achieve $\mathcal{O}(L^2)$ DOFs compared to $\mathcal{O}(L)$ offered by a ULA counterpart. One of the most studied sparse array structures is the coprime array [3] in which sensor locations are given by the union of those of a pair of uniform linear subarrays in which, for coprime integers M and N, one subarray consists of M elements placed with an inter-element spacing of N units and the other consists of N elements placed with an inter-element spacing of M units, where a unit is typically chosen as a half-wavelength.

By leveraging the concept of frequency diversity within the sparse array framework, a markedly greater number of DOFs can be attained [5–7]. Exploring the dependence of the steering vector on the signal carrier frequency gives rise to multi-frequency coprime arrays. These arrays construct a virtual coprime array using a single ULA and two or more continuous-wave sinusoids with frequencies adhering to a specific coprime relationship. Such an approach extends the concept of coprime arrays to a joint spatio-spectral domain, thereby providing high flexibility for designing arrays with an increased number of DOFs and a reduced system complexity.

The concept of utilizing multiple frequencies for coprime array design has been extended to multi-frequency sparse arrays. Different multi-frequency sparse array configurations and their performance, Cramer-Rao lower bound, and number of DOFs have been extensively studied in [8–15]. In particular, multi-frequency sparse array structures are designed in [12, 13, 15] such that the resulting difference coarrays are free of redundant lags and, as a result, achieve the maximum number of attainable DOFs. Nevertheless, while the frequency diversity-based approaches render high flexibility and an increased number of DOFs, the sensor locations of the physical antennas are rather restrictive such that the frequencies have a coprime relationship defined for integer numbers and all difference lags are integer multiples of the half-wavelength. Such a condition limits the choices for possible sensor locations and coprime frequencies. It often requires a large separation between the frequencies, making the array design challenging in some applications.

The recently developed concept of rational array design [16, 17] allows for successful detection of signals while the array sensors are located in non-integer locations. In this case, a subset of sensors deviate from the half-wavelength grid. The notion of rational arrays can be extended to multi-frequency sparse array design by exploiting frequencies that are coprime in the rational sense. A rational sparse array exploiting a ULA and multi-frequency signals is considered in [18] in which the virtual sensors and, subsequently, difference lags are located in non-integer positions. Compared to traditional multi-frequency sparse arrays, such rational array design provides great flexibility because the integer constraint for the sensor location or frequency pairs is no longer required. An important advantage of such multi-frequency rational sparse array design is that an array can now be designed with a small separation between the frequencies.

In this paper, the identifiability condition for rational sparse arrays exploiting rational coprime frequencies is addressed. Such a condition guarantees that, for any two distinct signal directions, the maximum spatial correlation coefficient is less than unity, that is, the DOA of the signal can be uniquely recovered from its steering vector and that type-1 spatial

This work was supported in part by the National Science Foundation (NSF) under grant No. ECCS-2236023.

ambiguity [19] is avoided. Furthermore, the applicability of direct MUSIC [20–22] for the detection of signals without false peaks is discussed.

Notations: We use lowercase (uppercase) bold characters to denote vectors (matrices). In particular, $\boldsymbol{I}_N$ denotes the $N \times N$ identity matrix. $(.)^{\mathrm{T}}$ and $(.)^{\mathrm{H}}$ respectively represent the transpose and conjugate transpose of a matrix or a vector. $\mathrm{diag}[\cdot]$ forms a diagonal matrix from a vector. $\gcd(a, b)$ and $\mathrm{lcm}(a, b)$ respectively denote the greatest common divisor (GCD) and the least common multiple (LCM) of two integers a and b. We use $\mathbb{C}^{M\times N}$ to denote the $M \times N$ complex space, and $\mathbb{Z}^+$ stands for the set of positive integers.

II. System Model

Consider a DOA estimation problem where $I \geq 2$ continuous-wave signals with frequencies f_i, where $i = 1,\ 2,\ \cdots,\ I$, are emitted from a single transmit antenna or a phased array. The signals are reflected by K far-field targets and impinge on an array consisting of N physical sensors which are located at

$$\mathbf{z}_0 = \{0,\ l_1,\ l_2,\ \cdots,\ l_{N-1}\}d, \tag{1}$$

where $l_1,\ l_2,\ \cdots,\ l_{N-1}$ are positive integers sorted in an increasing order and d is the interelement spacing of the physical array. The I carrier frequencies are related by

$$\frac{M_1}{f_1} = \frac{M_2}{f_2} = \cdots = \frac{M_I}{f_I} = \frac{2d}{c}, \tag{2}$$

where c denotes the propagation speed of electromagnetic waves in free space.

In multi-frequency sparse arrays considered in [12, 13, 15], it is assumed that M_i takes integer values so that $d = M_i\lambda_i/2$ is an integer multiple of half-wavelength in the respective frequency and, therefore, all virtual sensors are located on the half-wavelength grid. In this paper, we consider multi-frequency rational sparse arrays in which M_i as rational numbers such that $M_i = P_i/Q_i$, where P_i and Q_i are coprime integers [18]. Note that, multi-frequency integer coprime arrays become a special case of multi-frequency rational sparse arrays when the physical array is uniform linear and $Q_i = 1$ holds for all i.

Because $d = M_i c/(2f_i) = M_i\lambda_i/2$, the positions of the virtual sensors corresponding to frequency f_i are expressed as

$$\tilde{\mathbf{z}}_i = \{0,\ M_i l_1,\ M_i l_2,\ \cdots,\ M_i l_{N-1}\}\frac{\lambda_i}{2}. \tag{3}$$

Denoting the DOA of the k-th signal as θ_k, $k = 1, \cdots, K$, the received signal vector associated with the i-th frequency component is

$$\tilde{\boldsymbol{x}}_i(t) = e^{j2\pi f_i t}\sum_{k=1}^{K}\rho_k^{(i)}(t)\boldsymbol{a}_i(\theta_k) + \tilde{\boldsymbol{n}}_i(t), \tag{4}$$

where $\rho_k^{(i)}(t)$ is the reflection coefficient of the k-th target corresponding to the i-th frequency, which is in general frequency-dependent because both phase delay and target reflectivity vary with frequency. In addition,

$$\boldsymbol{a}_i(\theta_k) = \left[1,\ e^{-j\pi M_i l_1 \sin(\theta_k)}, \cdots, e^{-j\pi M_i l_{N-1}\sin(\theta_k)}\right]^{\mathrm{T}} \tag{5}$$

is the steering vector of the signal at θ_k corresponding to the i-th frequency and $\tilde{\boldsymbol{n}}_i(t) \sim \mathcal{CN}(0, \sigma_n^{(i)}\boldsymbol{I}_N)$ denotes the additive white Gaussian noise.

After demodulating the signal vector using carrier frequency f_i and denoting $\omega_k = \pi\sin(\theta_k)$, we obtain the baseband signal vector as

$$\boldsymbol{x}_i(t) = \sum_{k=1}^{K}\rho_k^{(i)}(t)\boldsymbol{a}_i(\omega_k) + \boldsymbol{n}_i(t) = \boldsymbol{A}_i\boldsymbol{s}_i(t) + \boldsymbol{n}_i(t), \tag{6}$$

where

$$\boldsymbol{a}_i(\omega_k) = \left[1,\ e^{-jM_i l_1\omega_k}, \cdots, e^{-jM_i l_{N-1}\omega_k}\right]^{\mathrm{T}}, \tag{7}$$

$\boldsymbol{A}_i = [\boldsymbol{a}_i(\omega_1), \boldsymbol{a}_i(\omega_2), ..., \boldsymbol{a}_i(\omega_K)]$ is the array manifold of the virtual array due to the i-th frequency, and $\boldsymbol{s}_i(t) = [\rho_1^{(i)}(t),\ ...,\ \rho_K^{(i)}(t)]^{\mathrm{T}}$.

By stacking the received data corresponding to all I frequencies, the received signal vector of the entire virtual array is obtained as

$$\begin{aligned}\boldsymbol{x}(t) &= \begin{bmatrix}\boldsymbol{x}_1(t)\\ \boldsymbol{x}_2(t)\\ \vdots\\ \boldsymbol{x}_I(t)\end{bmatrix} = \begin{bmatrix}\boldsymbol{A}_1\boldsymbol{s}_1(t)\\ \boldsymbol{A}_2\boldsymbol{s}_1(t)\\ \vdots\\ \boldsymbol{A}_I\boldsymbol{s}_I(t)\end{bmatrix} + \boldsymbol{n}(t)\\ &= \begin{bmatrix}\boldsymbol{A}_1\\ \boldsymbol{A}_I\tilde{\boldsymbol{D}}_2\\ \vdots\\ \boldsymbol{A}_I\tilde{\boldsymbol{D}}_I\end{bmatrix}\boldsymbol{s}(t) + \boldsymbol{n}(t) = \boldsymbol{A}\boldsymbol{s}(t) + \boldsymbol{n}(t),\end{aligned} \tag{8}$$

where $\boldsymbol{s}(t) = \boldsymbol{s}_1(t)$ and $\tilde{\boldsymbol{D}}_i = \mathrm{diag}[d_1^{(i)}, ..., d_K^{(i)}]$ with $d_k^{(i)} = \rho_k^{(i)}/\rho_k^{(1)}$. The effective steering vector of the k-th signal becomes

$$\boldsymbol{a}(\omega_k) = [\boldsymbol{a}_1^{\mathrm{T}}(\omega_k)\ \ d_k^{(2)}\boldsymbol{a}_2^{\mathrm{T}}(\omega_k)\ \cdots\ \ d_k^{(I)}\boldsymbol{a}_I^{\mathrm{T}}(\omega_k)]^{\mathrm{T}}. \tag{9}$$

In this paper, we only consider the scenario in which the reflection coefficient $\rho_k^{(i)}$ does not vary with frequency, i.e., $d_k^{(i)} = 1$ for all k and i. This is referred to as the proportional spectra scenario [23].

III. Identifiability Analysis and Direct MUSIC

Denoting $\bar{d}$ as half-wavelength in a normalized frequency sense, we rewrite (3) as

$$\mathbf{z}_i = \{0,\ M_i l_1,\ M_i l_2,\ \cdots,\ M_i l_{N-1}\}\bar{d}. \tag{10}$$

Then, the rendered multi-frequency rational sparse array corresponding to all I frequencies is given as

$$\mathbf{z} = \bigcup_{i=1}^{I}\mathbf{z}_i. \tag{11}$$

A. Condition for unique recovery of signal DOAs from its steering vector

In the previous section, we discussed how frequency diversity can be exploited to create a virtual sparse array. For simplicity and without loss of generality, consider two frequencies f_1 and f_2 such that $M_1/f_1 = M_2/f_2$. In this case, for physical sensor locations described in (1), the set of virtual sensor locations in (11) can be written as,

$$\mathbf{z} = \{0,\ M_1 l_1,\ \cdots,\ M_1 l_{N-1},\ M_2 l_1, \cdots,\ M_2 l_{N-1}\}\bar{d}. \quad (12)$$

It should be noted that the sensor locations in (12) are rational numbers consisting of integers as a special case. The GCD of any m positive rational numbers $r_i = U_i/V_i,\ i = 1, 2, \cdots, m$ with $U_i, V_i \in \mathbb{Z}^+\ \forall i$ is given by

$$\gcd(r_1, r_2, \cdots, r_m) = \frac{\gcd(U_1, U_2, \cdots, U_m)}{\mathrm{lcm}(V_1, V_2, \cdots, V_m)}. \quad (13)$$

As stated in [17], the set of m rational numbers r_1, r_2,$\cdots$, r_m are considered coprime if the GCD of the set is less than or equal to one. Therefore, the sensor locations of the virtual array in (12) are said to be coprime if $\gcd(M_1 l_1, \cdots, M_1 l_{N-1}, M_2 l_1, \cdots, M_2 l_{N-1}) \leq 1$. Furthermore, it is shown in [16, 27] that the coprimality of the sensor locations is a necessary and sufficient condition for the DOA of a signal to be uniquely identifiable from its steering vector, i.e., to avoid the type-1 spatial ambiguity. This condition for the unambiguous detection of the DOAs [24] implies that the spatial correlation coefficient γ is less than unity for $-\pi \leq \omega_l \neq \omega_k < \pi$, i.e., [25]

$$\gamma = \frac{1}{N}|\boldsymbol{a}^{\mathrm{H}}(\omega_l)\boldsymbol{a}(\omega_k)| < 1. \quad (14)$$

Therefore, for the case of multi-frequency rational arrays, we can have the following generalization:

Theorem 1: The necessary and sufficient condition for the signal DOA to be uniquely identifiable from its steering vector such that the spatial correlation coefficient $\gamma < 1$ for $-\pi \leq \omega_l \neq \omega_k < \pi$ is satisfied when

$$\gcd(M_1, M_2) \cdot \gcd(l_1, l_2, \cdots, l_{N-1}) \leq 1. \quad (15)$$

Proof. As stated previously, the necessary and sufficient condition for the unique recoverability of the signal DOA is the coprimality of the sensor locations, i.e.,

$$\gcd(M_1 l_1, \cdots, M_1 l_{N-1}, M_2 l_1, \cdots, M_2 l_{N-1}) \leq 1. \quad (16)$$

It is well known that the $\gcd(\cdot)$ function satisfies the distributive and associativity property. That is, for any positive numbers α_1, α_2, α_3, and α_4, $\gcd(\alpha_1\alpha_2, \alpha_1\alpha_3) = \alpha_1 \cdot \gcd(\alpha_2, \alpha_3)$ and $\gcd(\alpha_1, \alpha_2, \alpha_3, \alpha_4) = \gcd(\gcd(\alpha_1, \alpha_2), \gcd(\alpha_3, \alpha_4))$ holds true. Therefore, using the associative property to (16), we obtain

$$\gcd(\gcd(M_1 l_1, \cdots, M_1 l_{N-1}), \gcd(M_2 l_1, \cdots, M_2 l_{N-1})) \leq 1, \quad (17)$$

which can be further simplified using the distributive property as

$$\gcd(M_1 \cdot \gcd(l_1, l_2, \cdots, l_{N-1}), M_2 \cdot \gcd(l_1, l_2 \cdots, l_{N-1})) \leq 1. \quad (18)$$

Because $\gcd(l_1, \cdots, l_{N-1})$ is also a positive number, using the distributive property again, (18) simplifies to $\gcd(M_1, M_2) \cdot \gcd(l_1, l_2, \cdots, l_{N-1}) \leq 1$. This concludes the proof. □

It is noted that the extension of the unique identifiability condition for $I \geq 2$ frequencies is straightforward and is given as

$$\gcd(M_1, M_2, \cdots, M_I) \cdot \gcd(l_1, l_2, \cdots, l_{N-1}) \leq 1. \quad (19)$$

It is interesting to note that (19) allows optimal design of multi-frequency rational sparse arrays by decoupling the frequencies selection from that of sensor locations. Furthermore, condition (19) can be satisfied even by widely separated sparse physical arrays if the frequencies are appropriately chosen.

B. Unambiguous detection using direct MUSIC

It is shown in [26] that the MUSIC algorithm can identify K signals unambiguously and without any false peaks if and only if the $N \times K$ array manifold matrix

$$\mathbf{A} = [\boldsymbol{a}(\omega_1),\ \boldsymbol{a}(\omega_2), \cdots, \boldsymbol{a}(\omega_K)] \quad (20)$$

is rank K for all distinct ω_i in $0 \leq \omega_i < 2\pi$.

We now show that (20) is full rank K regardless of whether ω_{K+1} is distinct modulo $2\pi/M_1$ or $2\pi/M_2$ from any of the signals. Assume that ω_K is not distinct modulo $2\pi/M_1$ with any one of the signals, say ω_1 such that $\omega_K = \omega_1 + 2\pi h/M_1$, where $h \in \mathbb{Z}^+$, and thus $\boldsymbol{a}_1(\omega_1) = \boldsymbol{a}_1(\omega_K)$. In this case, the array manifold corresponding to the total virtual sparse array can be obtained from (8) as,

$$\mathbf{A} = \begin{bmatrix}\mathbf{A}_1 \\ \mathbf{A}_2\end{bmatrix} = \begin{bmatrix}\boldsymbol{a}_1(\omega_1) & \boldsymbol{a}_1(\omega_2) & \cdots & \boldsymbol{a}_1(\omega_K) \\ \boldsymbol{a}_2(\omega_1) & \boldsymbol{a}_2(\omega_2) & \cdots & \boldsymbol{a}_2(\omega_K)\end{bmatrix}. \quad (21)$$

Let us initially assume that $\mathbf{A}$ is not full rank and since $\boldsymbol{a}_1(\omega_1) = \boldsymbol{a}_1(\omega_K)$, there exists a non-zero vector $\boldsymbol{b} \in \mathbb{C}^K$ such that $\mathbf{A}_1\boldsymbol{b} = \mathbf{0}$. For $\mathbf{A}\boldsymbol{b} = \mathbf{0}$ to be true, $\mathbf{A}_2\boldsymbol{b} = \mathbf{0}$ must also be satisfied, which indicates that $\boldsymbol{a}_2(\omega_1) = \boldsymbol{a}_2(\omega_K)$. This is possible if and only if ω_K is not distinct modulo $2\pi/M_2$ with ω_1. Since M_1 and M_2 are coprime numbers, it is not possible for ω_K to be simultaneously distinct modulo $2\pi/M_1$ and distinct modulo $2\pi/M_2$ with ω_1 [22]. This implies that there is no non-zero vector $\boldsymbol{b}$ such that $\mathbf{A}\boldsymbol{b} = \mathbf{0}$, indicating $\mathbf{A}$ is indeed full rank regardless of whether ω_K is distinct modulo $2\pi/M_1$ or $2\pi/M_2$ with any of the signal locations ω_i. Therefore, using direct MUSIC on rational sparse arrays will resolve all signal locations without ambiguity.

IV. Simulation Results

In this section, we provide simulation results that demonstrate the justification for the conditions stated to avoid type-1 spatial ambiguity. Let us consider a sparse ULA with physical sensors located at integer positions $\mathbf{z}_0 = \{0,\ 2,\ 4,\ 6,\ 8\}d$. In

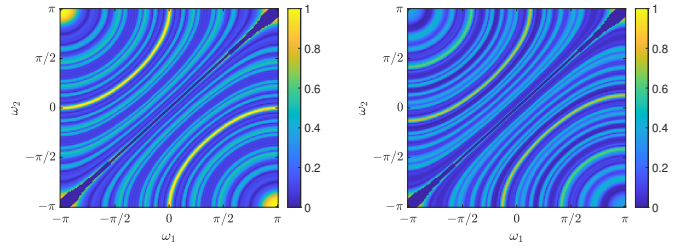

(a) Type-1 spatial ambiguity occurs (b) No type-1 spatial ambiguity

Fig. 1: Removal of type-1 spatial ambiguity by using rational sparse frequency pair since $\max(\gamma) < 1$.

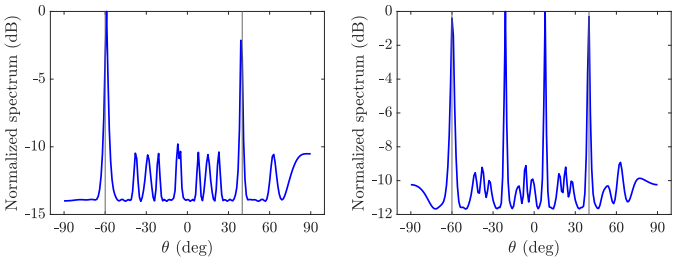

(a) No spatial aliasing occurs (b) Spatial aliasing occurs

Fig. 2: No spatial aliasing present in MUSIC spectrum for the rational coprime array

this case, the rendered multi-frequency rational sparse array is a multi-frequency sparse coprime array.

Fig. 1(a) shows the presence of type-1 spatial ambiguity as the GCD of the sensor locations is $\gcd(5,4)\cdot\gcd(2,4,6,8) = 2 > 1$ and does not satisfy the condition in (15). It is noted that the high correlation coefficients in the mainlobe region ($\omega_1 \approx \omega_2$) are removed from Fig. 1 to emphasize the spatial correlation coefficients in other regions. In comparison, if rational frequency pairs are chosen such that $M_1 = 5$ and $M_2 = 4.7 = 47/10$, then the GCD of the sensor location is obtained as $\gcd(5, 4.7) \cdot \gcd(2,4,6,8) = 1/5 < 1$ which satisfies the coprimality condition in (15). It can also be observed in Fig. 1 (b) that the type-1 spatial ambiguity is removed since the maximum correlation coefficient is now less than unity. It is also interesting to note that linear arrays with sensors placed along the half-wavelength grid show ambiguity in DOA estimation for the $(-\pi, \pi)$ DOA pairs as depicted in Fig. 1(a). On the other hand, when rational coprime arrays are used such ambiguity is overcome and the rational coprime array can successfully detect signals even from end-fire directions.

Fig. 2 shows the corresponding MUSIC spectra in which two signals arrive from $-60°$ and $40°$. It is observed in Fig. 2 that spatial alias only exists for the integer coprime array but not the rational coprime arras in this case. It is noted that the frequency separation for the rational coprime array is 6.2 % whereas that for the integer coprime array is 20.4%. Thus, when it comes to unambiguous DOA estimation with a reduced frequency separation, the multi-frequency rational coprime array provides much higher flexibility compared to traditional multi-frequency integer coprime arrays.

To confirm the applicability of direct MUSIC to rational coprime arrays, we consider an $N = 9$ element ULA and two frequencies f_1 and f_2 are chosen such that $M_1 = 5$ and $M_2 = 4.7$. The GCD of the sensor locations of the virtual coprime array can be calculated to be $1/10$ which is less than unity and thus satisfies the condition to avoid type-1 ambiguity. We consider $K = 6$ uncorrelated signals to be evenly distributed in $[-60°, 60°]$. The noise power at each frequency is assumed to be identical and the phase difference between the received signal corresponding to different frequencies is uniformly distributed in $[0, 2\pi]$. $T = 500$ snapshots are considered and the input SNR is set to 0 dB. It is observed in Fig. 3(a) that the six signals are resolved without unambiguous or false peaks by the rational coprime array using direct MUSIC. Fig. 3(b) shows the results of direct MUSIC on an integer coprime array when the two frequencies f_1 and f_2 are chosen such that $M_1 = 5$ and $M_2 = 4$. For this specific example, although the integer coprime array can also successfully detect all signals, its MUSIC spectrum has much higher sidelobe levels compared to the rational coprime array with a similar virtual aperture.

Fig. 3(c) shows the root mean-square error (RMSE) performance of the rational and integer coprime arrays with respect to the number of signals. The RMSE results are calculated using 200 independent trials. It is seen in Fig. 3(c) that the rational and integer coprime arrays have similar RMSE performance, but the rational coprime array can resolve one additional signal compared to the integer coprime array. This is due to the fact that, for the integer coprime array with $M_1 = 5$ and $M_2 = 4$, there is redundancy at lag 20, thus reducing the number of unique lags by one. On the other hand, the rational array is designed to achieve redundancy-free difference lags. It is noted that multi-frequency integer coprime arrays are more prone to lag redundancy due to the restricted number of integer lag positions.

V. Conclusion

In this paper, we considered the extension and generalization of the multi-frequency sparse array framework to rational arrays. We revealed that the coprimality of the multi-frequency rational sparse arrays can be decoupled into those of the frequencies and physical array configurations. Based on this observations, it became clear that unambiguous DOA estimation can be achieved by a sparse array provided that the frequencies are chosen to provide a small GCD. Simulation results are provided to verify the effectiveness of the multi-frequency rational coprime arrays and the analysis of the condition for achieving unambiguous DOA estimation.

VI. References

[1] T. E. Tuncer and B. Friedlander (Eds.), *Classical and Modern Direction-of-Arrival Estimation*, Academic Press, 2009.

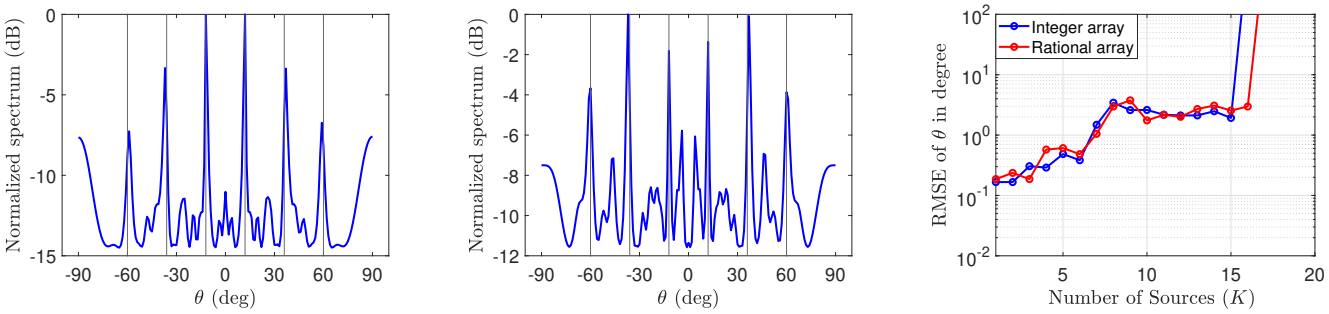

(a) Rational array ($M_1 = 5$, $M_2 = 4.7$). (b) Integer array ($M_1 = 5$, $M_2 = 4$). (c) RMSE vs. number of signals (K).

Fig. 3: Performance comparison of rational and integer coprime arrays.

[2] P. Pal and P. P. Vaidyanathan, "Nested arrays: A novel approach to array processing with enhanced degrees of freedom," *IEEE Trans. Signal Process.*, vol. 58, no. 8, pp. 4167–4181, Aug. 2010.

[3] P. P. Vaidyanathan, and P. Pal, "Sparse sensing with co-prime samplers and arrays," *IEEE Trans. Signal Process.*, vol. 59, no. 2, pp. 573–586, Feb. 2011.

[4] S. Qin, Y. D. Zhang, and M. G. Amin, "Generalized coprime array configurations for direction-of-arrival estimation," *IEEE Trans. Signal Process.*, vol. 63, no. 6, pp. 1377–1390, March 2015.

[5] Y. D. Zhang, M. G. Amin, F. Ahmad, and B. Himed, "DOA estimation using a sparse uniform linear array with two CW signals of co-prime frequencies," in *Proc. IEEE Int. Workshop Comput. Adv. Multi-Sensor Adaptive Process. (CAMSAP)*, Saint Martin, Dec. 2013, pp. 404–407.

[6] S. Qin, Y. D. Zhang, M. G. Amin, and B. Himed, "DOA estimation exploiting a uniform linear array with multiple co-prime frequencies," *Signal Process.*, vol. 130, pp. 37–46, Jan. 2017.

[7] A. Liu, X. Zhang, Q. Yang, and W. Deng, "Fast DOA estimation algorithms for sparse uniform linear array with multiple integer frequencies," *IEEE Access*, vol. 6, pp. 29952–29965, May 2018.

[8] S. Qin, Y. D. Zhang, and M. G. Amin, "DOA estimation exploiting coprime frequencies," in *Proc. SPIE*, vol. 9103, no. 91030E, Baltimore, MD, May 2014, p. 1–7.

[9] Y. Liu and J. R. Buck, "High-resolution direction-of-arrival estimation in SNR and snapshot challenged scenarios using multi-frequency coprime arrays," in *Proc. IEEE Int. Conf. Acoust., Speech Signal Process. (ICASSP)*, New Orleans, LA, March 2017, pp. 3434–3438.

[10] A. Ahmed, Y. D. Zhang, and B. Himed, "Cumulant-based direction-of-arrival estimation using multiple co-prime frequencies," in *Proc. Asilomar Conf. Signals, Syst., Computers,* Pacific Grove, CA, Oct. 2017, pp. 1188–1192.

[11] M. Guo, Y. D. Zhang, and T. Chen, "Performance analysis for uniform linear arrays exploiting two coprime frequencies," *IEEE Signal Process. Lett.*, vol. 25, no. 6, pp. 838–842, June 2018.

[12] S. Zhang, A. Ahmed, Y. D. Zhang, and S. Sun, "DOA estimation exploiting interpolated multi-frequency sparse array," in *Proc. IEEE Sensor Array and Multich. Signal Process. (SAM) Workshop*, Hangzhou, China, June 2020, pp. 1–5.

[13] A. Ahmed, D. Silage, and Y. D. Zhang, "High-resolution target sensing using multi-frequency sparse array," in *Proc. IEEE Sensor Array and Multich. Signal Process. (SAM) Workshop*, Hangzhou, China, June 2020, pp. 1–5.

[14] L. Liu, W. Wang, and M. Guo, "Performance analysis for DOA estimation using compressive measurements with coprime frequencies," *IEEE Sensors J.*, vol. 21, no. 6, pp. 8297–8309, March 2021.

[15] S. Zhang, A. Ahmed, Y. D. Zhang, and S. Sun, "Enhanced DOA estimation exploiting multi-frequency sparse array," *IEEE Trans. Signal Process.*, vol. 69, pp. 5935–5946, Oct. 2021.

[16] P. Kulkarni and P. P. Vaidyanathan, "Non-integer arrays for array signal processing," *IEEE Trans. Signal Process.*, vol. 70, pp. 5457–5472, 2022.

[17] P. Kulkarni and P. P. Vaidyanathan, "Rational arrays for DOA estimation," in *Proc. 2022 IEEE Int. Conf. Acoust., Speech Signal Process. (ICASSP)* , Singapore, 2022, pp. 5008–5012.

[18] Y. D. Zhang and M. G. Amin, "Multi-frequency rational sparse array for direction-of-arrival estimation," in *Proc. Int. Symp. Signals, Circuits and Systems*, Iași, Romania, July 2023, pp. 1–4.

[19] A. Manikas, *Differential Geometry in Array Processing*, Imperial College Press, 2004.

[20] R. O. Schmidt, "Multiple emitter location and signal parameter estimation," *IEEE Trans. Antennas Propagat.*, vol. 34, no. 3, pp. 276–280, March 1986.

[21] P. Pal and P. P. Vaidyanathan, "Coprime sampling and the music algorithm," in *Proc. Digital Signal Process. and Signal Process. Edu. Meet. (DSP/SPE)*, Sedona, AZ, 2011, pp. 289-294.

[22] P. P. Vaidyanathan and P. Pal, "Direct-MUSIC on sparse arrays," in *Proc. Internat. Conf. Signal Process. Commun. (SPCOM)*, Bangalore, India, 2012, pp. 1-5.

[23] E. BouDaher, Y. Jia, F. Ahmad, and M. G. Amin, "Multifrequency co-prime arrays for high-resolution direction-of-arrival estimation," *IEEE Trans. Signal Process.*, vol. 63, no. 14, pp. 3797–3808, 2015.

[24] Y. I. Abramovich, N. K. Spencer and A. Y. Gorokhov, "Resolving manifold ambiguities in direction-of-arrival estimation for nonuniform linear antenna arrays," *IEEE Trans. Signal Process.*, vol. 47, no. 10, pp. 2629-2643, Oct. 1999.

[25] H.-C. Lin, "Spatial correlations in adaptive arrays," *IEEE Trans. Antennas Propagat.*, vol. 30, no. 2, pp. 212–223, March 1982.

[26] P. Stoica and A. Nehorai, "MUSIC, maximum likelihood, and Cramer-Rao bound," *IEEE Trans. Acoust., Speech, Signal Process.*, vol. 37, no. 5, pp. 720–741, May 1989.

[27] P. P. Vaidyanathan and P. Pal, "Why does direct-MUSIC on sparse-arrays work?" in *Proc. Asilomar Conf. Signals, Systems and Computers*, Pacific Grove, CA, 2013, pp. 2007–2011.